

## Influence of particle packing on fracture properties of concrete

Huan He<sup>\*1,2</sup>, Piet Stroeven<sup>1</sup>, Martijn Stroeven<sup>1</sup> and Lambertus Johannes Sluys<sup>1</sup>

<sup>1</sup>Faculty of Civil Engineering and Geosciences, Delft University of Technology, Delft, The Netherlands

<sup>2</sup>Faculty of Applied Sciences, University of Liège, Liège, Belgium

(Received October 14, 2010, Revised January 7, 2011, Accepted January 8, 2011)

**Abstract.** Particle packing on meso-level has a significant influence on workability of fresh concrete and also on the mechanical and durability properties of the matured material. It was demonstrated earlier that shape exerts but a marginal influence on the elastic properties of concrete provided being packed to the same density, which is not necessarily the case with different types of aggregate. Hence, elastic properties of concrete can be treated as approximately structure-insensitive parameters. However, fracture behaviour can be expected structure-sensitive. This is supported by the present study based on discrete element method (DEM) simulated three-phase concrete, namely aggregate, matrix and interfacial transition zones (ITZs). Fracture properties are assessed with the aid of a finite element method (FEM) based on the damage materials model. Effects on tensile strength due to grain shape and packing density are investigated. Shape differences are shown to have only modest influence. Significant effects are exerted by packing density and physical-mechanical properties of the phases, whereby the ITZ takes up a major position.

**Keywords:** particle packing; particle shape; fracture properties; FEM; DEM; ITZ; concrete.

---

### 1. Introduction

Strength and fracture behaviour are regarded as important properties of concrete that are at the basis of structure design and analysis of this material. This field is extensively covered by experimental studies that mainly focus on influences exerted by aggregate type (Tschegg *et al.* 1995, Akçaoğlu *et al.* 2004, Yaşar *et al.* 2004, Chen and Liu 2004, Rocco and Elices 2008, 2009, Tabsh and Abdelfatah 2009), by *w/c* (Yaşar *et al.* 2004), and by loading concept (Tschegg *et al.* 1995, Yan and Lin 2006), whereby all structure-sensitive properties reveal size effects (van Vliet and van Mier 1999, Carpinteri *et al.* 2004, Stroeven 1973, Almusallam *et al.* 2004), etc.

Compared with time-consuming experiments, numerical modelling constitutes a more flexible and economic alternative. Numerical fracture models of concrete can be sub-divided into several groups such as continuum, discontinuous (based on extended finite element method, XFEM), discrete element and lattice models (Lilliu 2007). Continuum models conceive stress and strain as continuous throughout the material and include cracks smeared out over a region (crack band). As an example, a damage variable  $\omega$  is employed in continuum damage models to specify deterioration of the stiffness matrix (Stroeven 1973, Peerlings 1999, Jirásek and Patzák 2002). Non-local and gradient damage models are developed to resolve mesh sensitivity and damage localization (Brekelmans and Ayyapureddi 1995, Peerlings 1999, Jirásek and Marfia 2005, Ferrara and Di Prisco 2001). Discontinuous models

---

\* Corresponding author, Postdoctoral Fellow, E-mail: H.He@live.com

based on XFEM (Wells and Sluys 2001) are used to model cracks that can arbitrary run through a mesh in a mesh-objective manner. Discrete models treat materials as consisting of a numbers of rigid bodies. The force-displacement bond is applied for neighboured particles (Vonk 1992, Azevedo and Lemos 2005, 2006a, 2006b, Azevedo *et al.* 2010). Lattice models separate the material into a number of beams or trusses (Herrmann *et al.* 1989, Bažant *et al.* 1990, Leite *et al.* 2004). A purely linear elastic-brittle constitutive law can be applied to each beam in the lattice model (Schlangen and Garboczi 1997, Lilliu 2007).

Concrete is a heterogeneous particulate material that can be treated as a three-phase composite on meso-level. As the weakest part of normal concrete, the ITZ is regarded as the most feasible part for crack initiation and propagation. So, ITZs will play an important role in fracture behaviour of concrete. On the other hand, aggregate takes up to three quarters of concrete's volume, so it also strongly governs its mechanical properties. Shape is an important but complex property of the aggregate; hence grains are conventionally assumed spherical in numerical fracture analysis (Bažant *et al.* 1990, Azevedo and Lemos 2005, Zhao and Hao 2008). Despite its particulate nature, only limited information is provided in literature on effects on concrete's fracture behaviour due to particle packing (Du and Sun 2007, Rocco and Elices 2009).

This study will therefore focus on effects exerted by shape and packing of aggregate on concrete's fracture behaviour. Model concretes were simulated for this purpose on meso-level by DEM, and thereupon subjected to numerical fracture simulation approaches. This will allow drawing conclusions as to the aforementioned parameters, as well as to some additional mechanical and geometric properties of the three phases.

## 2. Experiments

Generally, a similar procedure is followed for the generation of numerical models of the three-

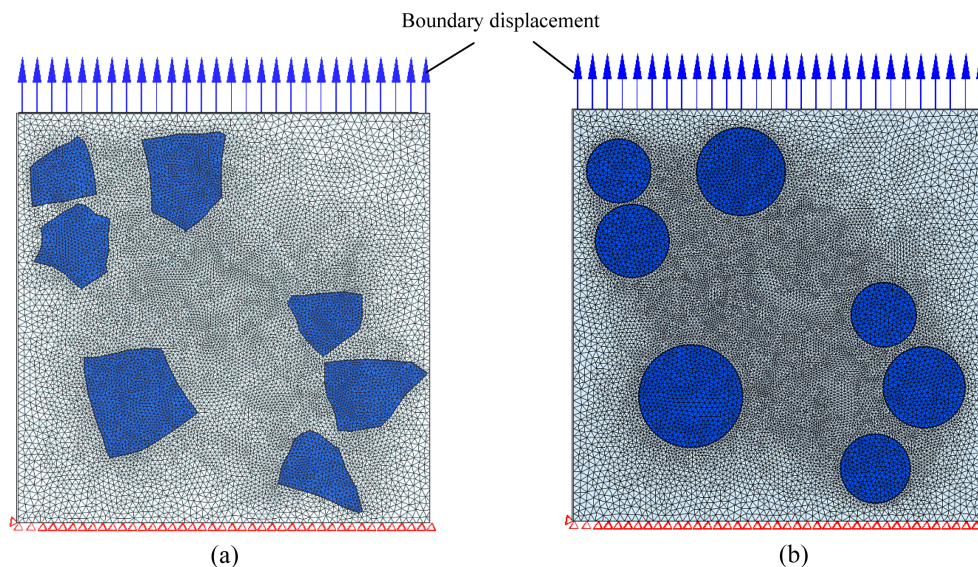


Fig. 1 Models with inclusions of different shape: (a) angular and (b) circular, meshed by GMSH

Table 1 Material properties of different phases applied in FEM ( $E$ ,  $\mu$  and  $\sigma_t$  represent Young's modulus, Poisson's ratio and tensile strength, respectively)

Components	$E$ (GPa)	$\mu$ (-)	$\sigma_t$ (MPa)
Aggregate	75	0.15	40
ITZ	7.2	0.35	2.2
Matrix	12	0.25	6

phase concrete structure as described in He *et al.* (2009). DEM is suitable for the generation of the granular structure of concrete (Stroeven *et al.* 2009). Therefore, a concurrent algorithm-based DEM system was used in this study (He 2010). A couple of meshed 2D examples obtained by sectioning the 3D DEM produced model concrete containing differently shaped inclusions are shown in Fig. 1. Such meshed models will then be transferred to the FEM system, so as to establish a numerical 2D concrete model. Compared with the aforementioned study of the elastic properties, a finer mesh is necessary to achieve better fracture simulation results. Basic material properties are assigned to the different phases, partly according to Li *et al.* (2003) adopting experimental results of Stock *et al.* (1979) and Kwan *et al.* (1999) as listed in Table 1. ITZs are fully described in accordance with geometric information by the small “weak” elements between aggregate and matrix. The model is subjected to the simple boundary conditions shown in Fig. 1. Later, when the influences exerted by the different parameters are discussed, this basic material model will be used as “reference”.

### 3. Damage material model

In this study, a simple isotropic damage model (Stroeven 1973, Jirásek and Marfia 2005, Radtke *et al.* 2008) will be applied for the description of the mechanical behaviour of each concrete phase. The model describes the stress-strain behaviour of a material in which damage evolution takes place, such as expressed by Eq. (1) and Fig. 2.

$$\sigma = (1 - \omega)\mathbf{D}\varepsilon \quad (1)$$

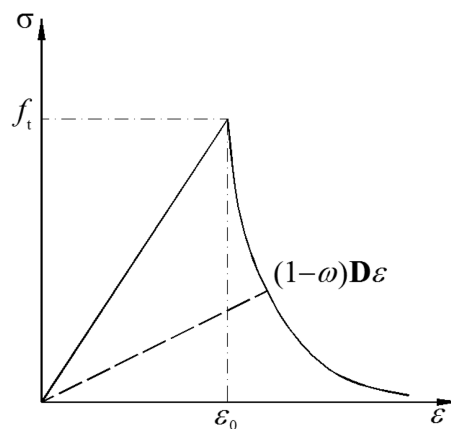


Fig. 2 Stress-strain relationship of the damage model

in which  $\sigma$  and  $\varepsilon$  define stress and strain of the material, respectively;  $\mathbf{D}$  is the stiffness matrix of the undamaged material;  $\omega$  is a damage scalar as defined by

$$\omega = \begin{cases} 0 \\ 1 - \frac{\varepsilon_0}{k} \exp\left(-\frac{k - \varepsilon_0}{\varepsilon_f - \varepsilon_0}\right) \end{cases} \quad (2)$$

where  $\varepsilon_0$  is the strain at peak stress,  $\varepsilon_0 = f_t/E$ , in which  $f_t$  and  $E$  are the tensile strength and elasticity modulus, respectively;  $\varepsilon_f$  is a parameter specifying the slope of the softening branch;  $k$  is a parameter related to the history of damage evolution.

The damage energy release rate  $Y$  is evaluated by means of the equivalent strain  $\tilde{\varepsilon}$

$$\tilde{\varepsilon} = \sqrt{\frac{2Y}{E}} \quad (3)$$

in which  $Y = \varepsilon^T \mathbf{D} \varepsilon$ . To solve the mesh sensitivity problem of the isotropic damage model, energy regularization (Brekelsmans and Ayyapureddi 1995, Radtke *et al.* 2008) is applied, with  $\varepsilon_f$  defined by

$$\varepsilon_f = \frac{\lambda}{h} \left( \varepsilon_f - \frac{\varepsilon_0}{2} \right) + \frac{\varepsilon_0}{2} \quad (4)$$

Herein,  $\lambda$  is defined as the width of the damage zone and  $h$  is a parameter related to the element size.

## 4. Parameter study

### 4.1 Mesh sensitivity checked by a simple planar model

Mesh sensitivity is an inherent problem of traditional local damage models, so that reliability of numerical simulation largely depends on mesh fineness. As indicated before, an energy regularization method is applied for solving this problem. The efficiency of the resulting improvement is checked by a simple planar model shown in Fig. 3. The model is also composed of three phases, i.e. aggregate, ITZ and matrix, in a series arrangement. The material properties of the three phases comply with Table 1. Information on size, dimensions, loading and boundary conditions is given in Fig. 3. A slightly weaker section is designed in the middle of the ITZ region for triggering crack

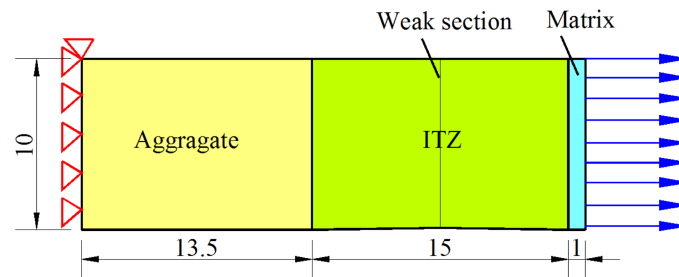


Fig. 3 Simple planar model to check mesh sensitivity of the material model (dimensions in mm)

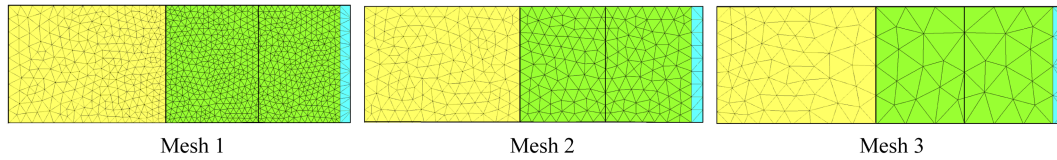


Fig. 4 Mesh of different fineness superimposed on the simple three-phase planar structure of Fig. 3

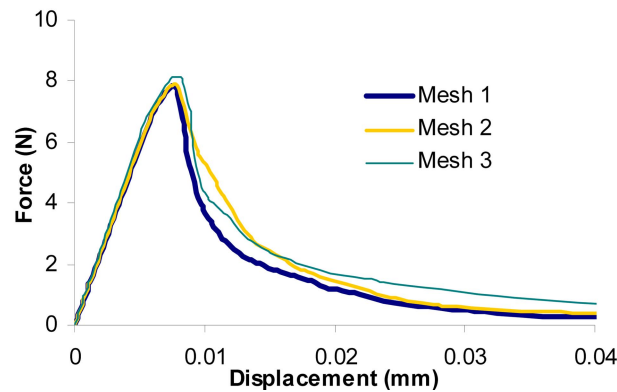


Fig. 5 F-D curves of the simple planar analyzed with different mesh fineness when subjected to uniaxial tension

initiation. Mesh fineness is varied in this planar model as shown in Fig. 4. These three planar models are subjected to uniaxial tension.

The most important results of the tensile tests are the force-displacement (F-D) curves presented in Fig. 5. The F-D curves of the three models are reasonably similar, despite the relatively large differences in mesh fineness; the softening curves of the three models form a narrow band. Therefore, the adopted material damage model for fracture evaluation is considered suitable for this study.

#### 4.2 Influence of shape and packing density of aggregate

As prime target, the influences exerted by shape and packing density of aggregate on fracture behaviour will be evaluated. Meso-structure models with different volume fraction and shape of aggregate as shown in Table 2 were used in the uniaxial tensile test, similar as in the approach to the elastic properties (He *et al.* 2009). Material properties of each phase comply with Table 1. The width of the ITZ is also maintained at 50  $\mu\text{m}$ . As the elastic behaviors has been studied in previous study (He *et al.* 2009), this paper will focus on post-peak (softening) fracture behavior of modeled concrete. Resulting post-peak F-D curves of the various models are presented in Fig. 6, where  $A_{aa}$  and  $A_{ac}$  represent the area fraction of aggregate in the model with arbitrary angular shape particles and with circular shaped ones, respectively.

The results of Fig. 6 demonstrate that models with circular-shaped aggregate reveal relatively high tensile strength as compared to models with angular-shaped inclusions. This may be due to the high stress concentrations in the case of angular-shaped inclusions, which leads to an earlier crack initiation and development. Similar results were found by Du and Lin (2007) in a numerical comparison of models with polygonal and spherical aggregate. However, distributions of polygonal

Table 2 Meso-material models in which different volume fractions (left to right) and different shapes of aggregate (top to bottom) were employed. Dispersion in comparable cases is similar

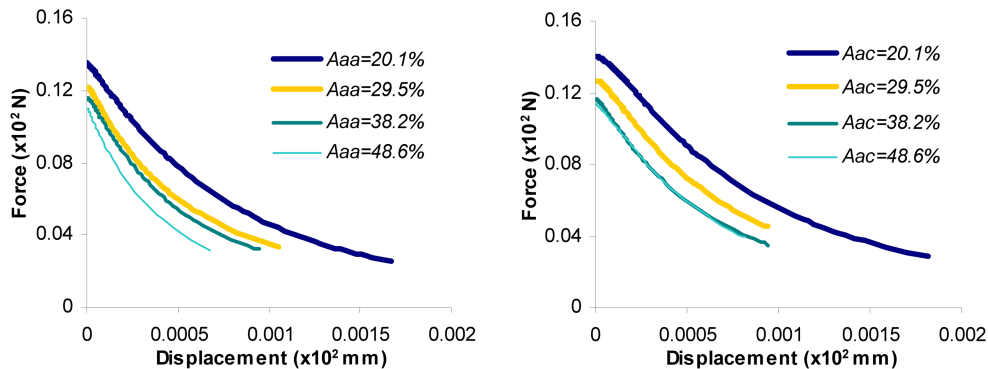
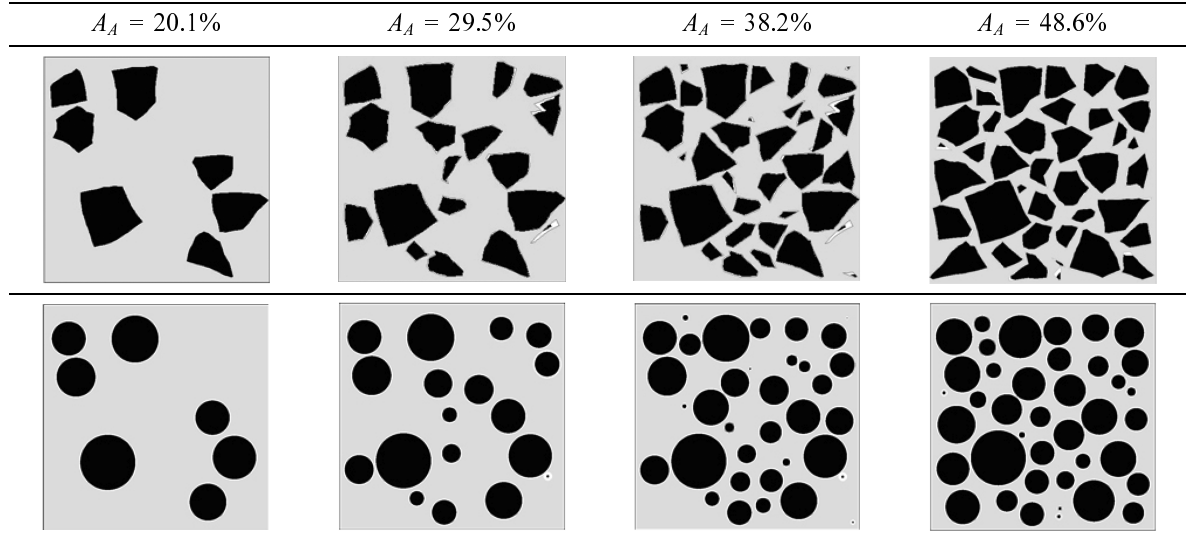


Fig. 6 Post-peak force-displacement curves of models containing different volume fraction of aggregate with angular shape (left) and with circular shape (right)

and spherical aggregate particles were in their study different in comparable situations, which may have affected their results. Therefore, this study will focus more explicitly on this issue. Some experimental results show tensile strength of concrete weakly depending on aggregate shape (Rocco and Ellices 2009). But it should be pointed out that experimental results are influenced by other factors, such as aggregate surface texture, different bonding capacity, strength of ITZ, etc. Hence, the numerical analysis can offer a more complete picture on the issue.

Fig. 7 shows the vertical displacement contours of models with the same aggregate volume density of 20.1%, however containing aggregate with different shape. Cracks are clearly delineated by the boundary between different colors. The figures indicate that cracks were first initiated in the relatively weak ITZs. Next, cracks propagate into the matrix to coalesce, forming the major crack in the model. The major cracks are roughly perpendicular to the loading direction and quite similar but not identical in the two models. The latter reflects the larger perimeter length versus area ratio,  $L_A$ ,

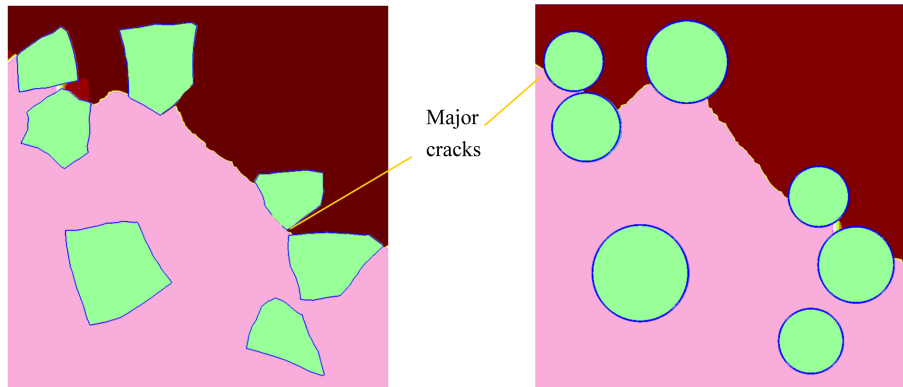


Fig. 7 Vertical displacement contour in model with angular aggregate (left) and spherical aggregate (right) (displacement declines from dark red to light red; line between major dark and light delineates the major crack; aggregate is depicted)

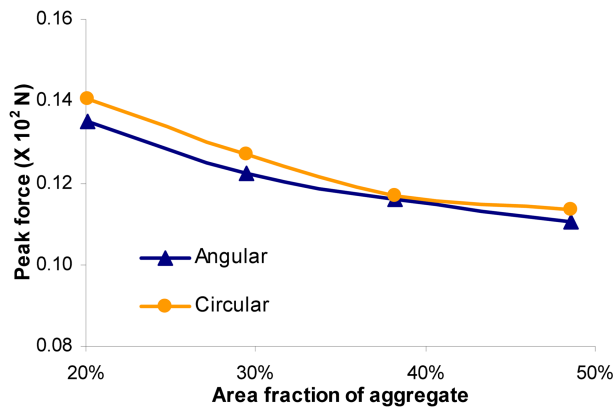


Fig. 8 Ultimate tensile strength of models containing aggregate with different shape at different volume fractions

of the angular aggregate, allowing the crack to follow ITZs over a somewhat longer distance. As a consequence, this effect can be expected augmented at larger particle densities.

Fig. 6 reveals the reduction of the tensile strength at increasing packing density of both angular and circular aggregate grains. This results from increased numbers of ITZ regions at higher packing density of aggregate. This promotes propagation and coalescence of cracks. Similar results on compression strength were found by Tasdemir and Karihaloo (2001). The results for different models are presented in Fig. 8, revealing at increasing packing density the different rates of strength decline for the two grain shapes.

It should be mentioned here that the tendencies obtained in the simulations largely depend on the properties of the ITZ. Fracture characteristics will change when the ITZ properties are modified with respect to those of the other phases, as will be discussed later. Still, a simple example in which the mechanical properties of the ITZ in the meso-structure models are taken similar to those of the matrix, may support the argument. The material basically reduces to a two-phase material. When concrete is upgraded in the high performance concrete (HPC) range, the ITZ will be disproportionately improved, so the simulated case is a realistic one. The post-peak F-D curves for this case are presented in Fig. 9, evidencing the significant impact of the ITZ on fracture behaviour of concrete.

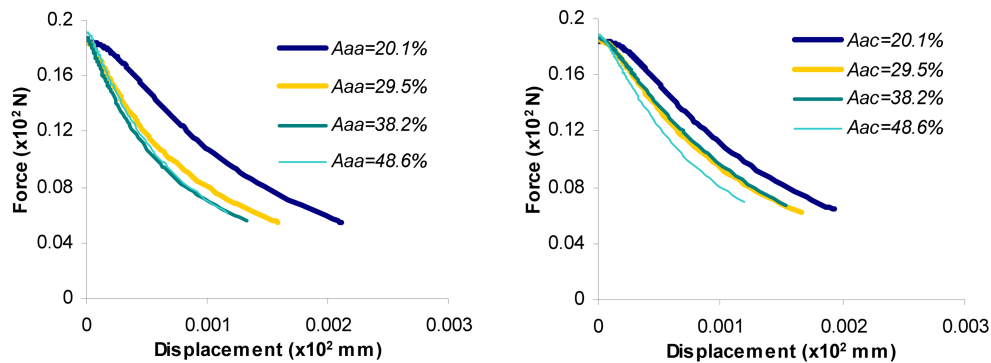


Fig. 9 Post-peak F-D curves of two-phase models (matrix + aggregate) at different volume fractions of aggregate, which consists of angular-shaped grains (left) or circular-shaped ones (right)

Obviously, shape of aggregate has a smaller influence on fracture behaviour when the ITZ is omitted. The effect of ITZ's mechanical properties will be more elaborately discussed. The tensile strength is slightly increased with increasing packing density of the aggregate. Hence, an opposite conclusion can be drawn in models without and with ITZ. Gradual improvement of the relative quality of the ITZ will be reflected, as a consequence, by a gradual transfer from behaviour depicted in Figs. 6 and 9.

#### 4.3 Influence of mechanical properties of aggregate

Firstly, the mechanical properties of the major component of concrete, i.e. aggregate will be emphasized. Later, influences exerted by other parameters such as the mechanical and geometric properties of the various phases will be assessed. For that purpose, a basic model containing 42.7% by volume of arbitrary-shaped aggregate is selected, as shown in Fig. 10. Different mechanical properties are applied to the same meso-structure model. Next, these models are subjected to the tensile test. The material properties of aggregate are listed in Table 3.

The post-peak F-D curves pertaining to the models with different mechanical properties of aggregate are

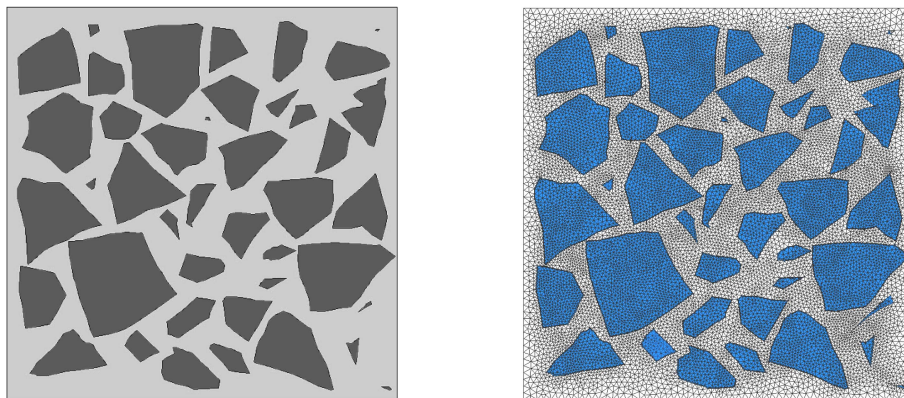


Fig. 10 Basic model ( $A_A = 42.7\%$ ) selected for evaluation of parameter influences: geometric model (left) and meshed model (right)

Table 3 Mechanical properties of aggregate used for comparison purposes in models

$(E_{agg}/E_{matrix})$	$E_{agg}$ (MPa)	$\sigma_t$ (MPa)
6.25	75	40
5	60	32
3	36	19
1	12	6

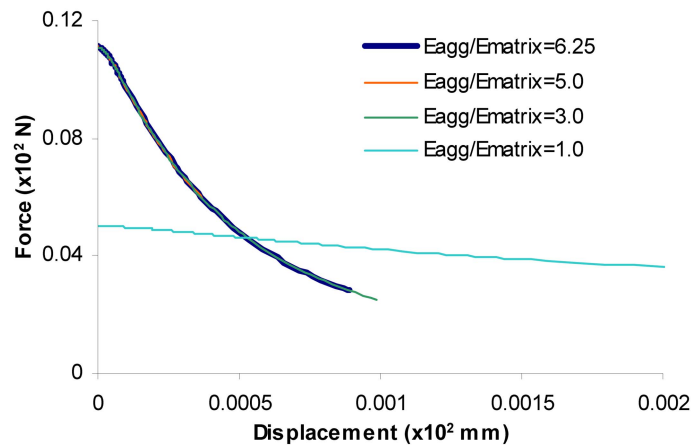


Fig. 11 Post-peak F-D curves of model concrete of Fig. 10 for different mechanical properties of the aggregate

shown in Fig. 11. The results indicate that the mechanical properties of the aggregate have only minor influence on the fracture behaviour of concrete as long as the aggregate is stronger than the matrix. This is because aggregate grains are rarely cracked when stronger than the matrix. But when the mechanical properties are equivalent with respect to those of the matrix, the tensile strength drops dramatically.

#### 4.4 Influence of ITZ's width

The influence on fracture behaviour exerted by ITZ's properties can be significant as shown before; therefore, its extension should also be considered a crucial feature of which effects on fracture properties should be carefully studied. Unfortunately, extension cannot easily be assessed in true experiments. Further, the width of the ITZ ( $W_{ITZ}$ ) depends on the sensitivity to particle configuration of the descriptor of material structure (Freudenthal 1950, Hu and Stroeven 2004). Zheng (2000) found analytically that the ITZ's width will be in a range of tens of micrometers in concrete in agreement with experimental findings (Scrivener and Nematì 1996). However, the ITZ is frequently assumed hundreds of micrometers wide in numerical simulations because of inherent difficulties (Lilliu 2007, Zhou and Hao 2008). Thus, it should be considered interesting and highly relevant to assess the influence of ITZ's width on fracture behaviour of concrete.

The basic model shown in Fig. 10 was used for this purpose, however with imposed variation in ITZ's width. Various widths were described by different numbers or sizes of interface elements. So, four different models with ITZ's width ranging from 30  $\mu\text{m}$  to 90  $\mu\text{m}$  were generated. These models were thereupon subjected to the tensile test. The obtained post-peak F-D curves and final

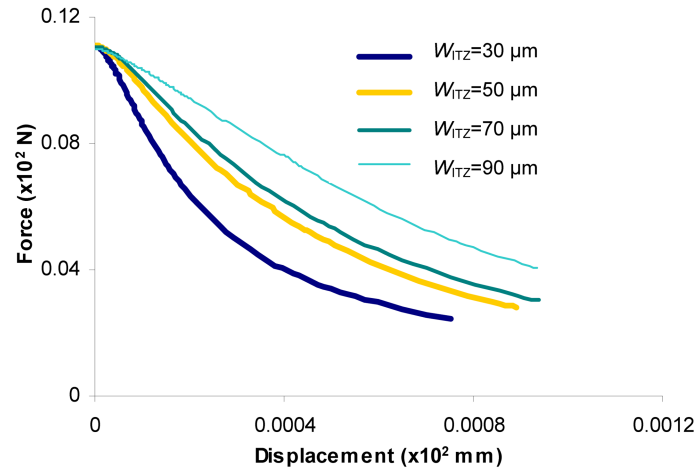


Fig. 12 Post-peak F-D curves of models with similar aggregate structure, however with ITZs having different widths

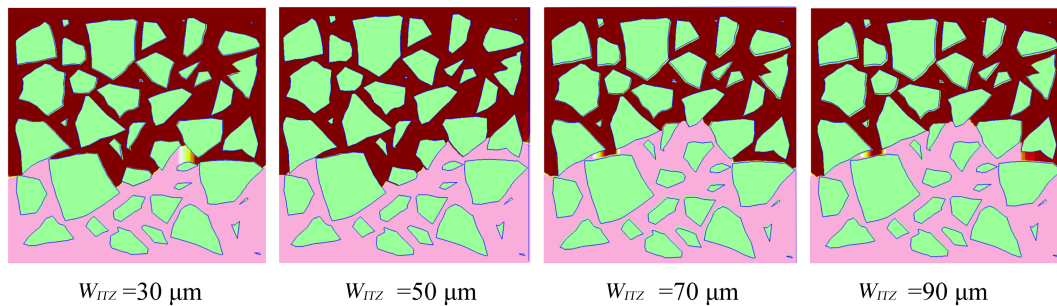


Fig. 13 Vertical displacement contour at ultimate reveals crack paths at different ITZ width

vertical displacement contours of different models are presented in Figs. 12 and 13, respectively.

Obviously, the width of the ITZ has a significant influence on fracture behaviour of concrete, which is particularly apparent in the softening range. A larger width of the ITZ gives rise to more ductile behaviour and marginally lower ultimate tensile strength. In other words, a three-phase model with more extensive ITZ has enhanced energy dissipation capacity. This is due to the changes in the crack paths and so changes of the damage patterns and increased ITZ length, as illustrated in Fig. 13. A similar study was conducted by Lilliu (2007), in which a lattice model was used. Different ITZ widths were selected from 250  $\mu\text{m}$  to 1000  $\mu\text{m}$  (Lilliu 2007), i.e. significantly exceeding more realistic values considered in our case. The results reveal that the model with wider ITZ has a more ductile behaviour and lower tensile strength (Lilliu 2007).

#### 4.5 Influence of mechanical properties of ITZ

Mechanical properties of the ITZ are directly related to the microstructure of the material. Different design parameters such as  $w/c$ , hydration duration, cement quality or cement blending will result in differences in material structure and thus in mechanical properties of the ITZ (Hu and Stroeven 2004). Hence, different mechanical properties are assigned to the basic model in Fig. 10 to assess its

Table 4 Different mechanical properties of ITZ employed in models for comparison purposes

$(E_{itz}/E_{matrix})$	$E_{itz}$ (MPa)	$\sigma_t$ of ITZ (MPa)
0.4	4.8	1.0
0.6	7.2	2.2
0.8	9.6	4.1
1.0	12.0	6.0

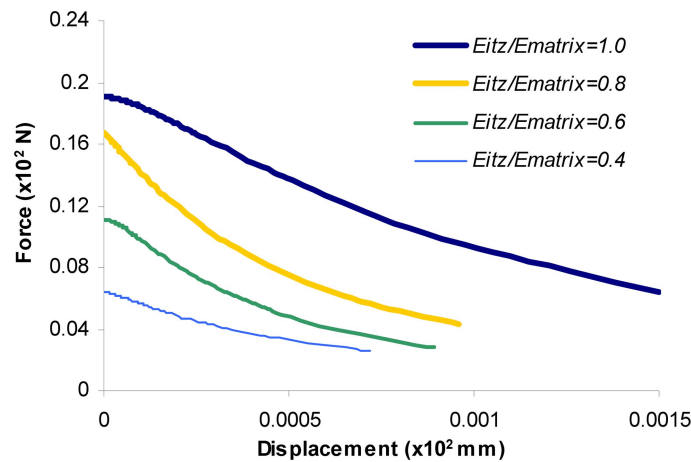


Fig. 14 Post-peak F-D curves of models in which ITZ's mechanical properties are varied

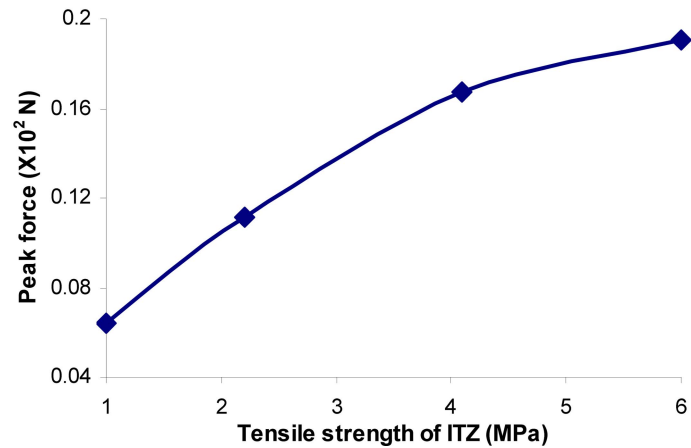


Fig. 15 Peak tensile force of models in which the tensile strength of the ITZ was varied

effect on the fracture behaviour of concrete. The proposed material properties of the ITZ are assumed proportional to the properties of the matrix; data are listed in Table 4.

Obtained models are then subjected to a tensile test. Corresponding post F-D curves are presented in Fig. 14, demonstrating the mechanical properties of the ITZ to have a dominant influence on tensile fracture behaviour of concrete. Better tensile performance of concrete is resulting from model material with improved ITZ properties. The relationship of the peak tensile force of concrete with tensile strength of the ITZ is plotted in Fig. 15.

Fig. 15 indicates concrete's tensile strength to gradually increase with increasing tensile strength of the ITZ. A similar conclusion can be found in the numerical study based on a lattice model by Lilliu (2007). However, promoting mechanical properties of the ITZ goes conventionally hand in hand with doing so for the matrix; this will be the case when reducing  $w/c$ . A disproportional improvement in ITZ density can be obtained by properly designed blending of the cement (Bui *et al.* 2005, Goldman and Bentur 1995).

#### 4.6 Influence of mechanical properties of matrix

Mechanical properties of the matrix, as with the ITZ, rely on the technological design parameters and curing conditions. Again, the model of Fig. 10 is used to identify the influence of mechanical properties of the matrix on fracture behaviour of concrete. Different material properties are assigned to the matrix in terms of aggregate to matrix stiffness ratios, as shown in Table 5. In case I, the properties of the ITZ are maintained on 60% level with respect to those of the matrix; in case II, the ITZ properties are kept constant. Case I therefore reveals the combined effect of matrix and ITZ on fracture behaviour. A mutual comparison of both cases will give insight in the separate effects exerted by matrix and ITZ on fracture behaviour of concrete.

Resulting post-peak F-D curves in different situations are shown in Fig. 16. It illustrates that the peak force value (and thus ultimate strength) of concrete increases dramatically when mechanical

Table 5 Different mechanical properties of matrix and ITZ used in models for comparison study

$E_{agg}/E_{matrix}$	$E_{matrix}$ (MPa)	$\sigma_t$ of matrix (MPa)	$E_{itz}$ (MPa)	$\sigma_t$ of ITZ (MPa)
6.25	12	6	7.2	2.2
5	15	14	9 (case I) 7.2 (case II)	7.5 (case I) 2.2 (case II)
3	25	27	15 (case I) 7.2 (case II)	14.4 (case I) 2.2 (case II)
1	75	40	45 (case I) 7.2 (case II)	21.3 (case I) 2.2 (case II)

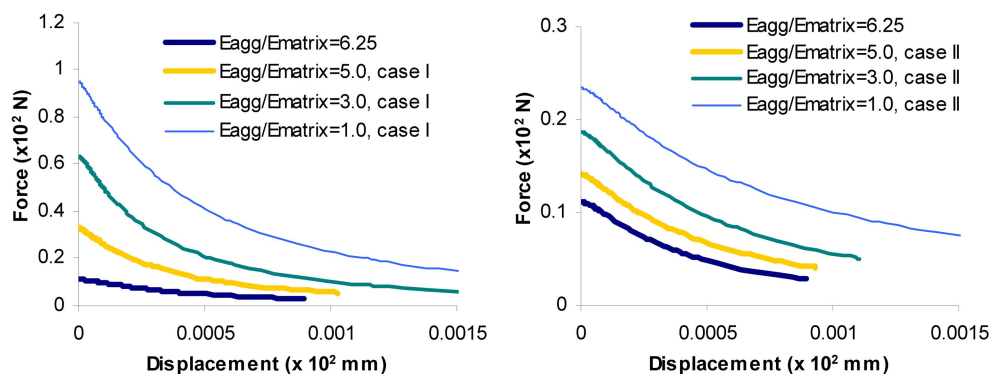


Fig. 16 Post-peak F-D curves of models in which mechanical properties of matrix and ITZ are proportionally varied (case I: left) and in which only those of the matrix are varied (case II: right)

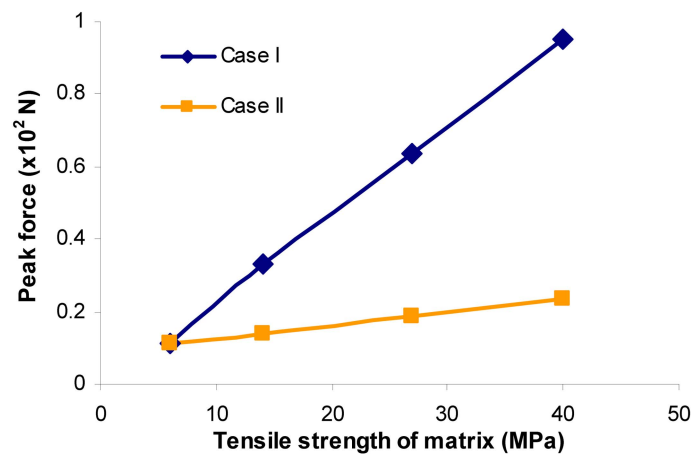


Fig. 17 Peak force of models in which mechanical properties of matrix and ITZ are varied (case I: proportional modifications in matrix and ITZ, case II: only modifications in matrix)

properties of matrix and associated ITZ are improved (case I). This peak force value will undergo but a moderate increase when only mechanical properties of the matrix are improved (case II). Peak force values in both cases are shown in Fig. 17 as function of the mechanical properties of the matrix. This demonstrates the paramount importance of upgrading both matrix and ITZ, or - as shown earlier - even disproportionately improving the ITZ.

## 5. Conclusions

Fracture behaviour of model concrete was analyzed in this study on meso-level, whereby influences of aggregate shape and packing on fracture behaviour were investigated. The results show that particle shape has modest influence on the tensile strength of concrete. Concrete with arbitrary angular shaped inclusions will have a lower tensile strength as compared to models with spherical aggregate grains, at similar packing density. This is due to higher stress concentrations near the aggregate and a larger proportion of relatively weak ITZ's. Higher packing density of aggregate was found leading to reduced tensile strength of normal concrete. Disproportionately improving the ITZ, as occurring in HPC range, will give rise to other conclusions. For normal weight concrete, the mechanical properties of the aggregate will have insignificant influence on fracture behaviour; cracks are conventionally initiated in the ITZ or in the matrix. ITZ has a dominant influence on tensile fracture behaviour of normal concrete. A larger width of the ITZ will result in a more ductile softening behaviour of concrete and at a marginally lower tensile strength. The tensile strength of concrete is significantly increased at improved properties of the ITZ. When the ITZ is proportionally improved with the matrix, this effect is more modest than when ITZ is disproportionately improved, e.g. in the HPC range at low  $w/c$ , or by well-designed cement blending. Hence, the ITZ is the most crucial factor affecting fracture of concrete.

## Acknowledgements

The authors would like to thank Ir. F.K.F. Radtke and Dr. Z. Guo for their significant cooperation and valuable discussions on the fracture behavior of concrete and this manuscript.

## References

- Akçaoğlu, T., Tokyay, M. and Çelik, T. (2004), "Effect of coarse aggregate size and matrix quality on ITZ and failure behavior of concrete under uniaxial compression", *Cement Concrete Compos.*, **26**(6), 633-638.
- Almusallam, A.A., Beshr, H., Maslehuddin, M. and Al-Amoudi, O.S.B. (2004), "Effect of silica fume on the mechanical properties of low quality coarse aggregate concrete", *Cement Concrete Compos.*, **26**(7), 891-900.
- Azevedo, N.M. and Lemos, J.V. (2005), "A generalized rigid particle contact model for fracture analysis", *Int. J. Numer. Anal. Meth. Geomech.*, **29**(3), 269-285.
- Azevedo, N.M. and Lemos, J.V. (2006a), "Hybrid discrete element/finite element method for fracture analysis", *Comput. Meth. Appl. Mech. Eng.*, **195**(33-36), 4579-4593.
- Azevedo, N.M. and Lemos, J.V. (2006b), "Aggregate shape influence on the fracture behaviour of concrete", *Struct. Eng. Mech.*, **24**(4), 411-427.
- Azevedo, N.M., de Lemos, J.V. and de Almeida, J.R. (2010), "A discrete particle model for reinforced concrete fracture analysis", *Struct. Eng. Mech.*, **36**(3), 343-361.
- Bažant, Z.P., Tabbara, M.R., Kazemi, M.T. and Pijaudier-Cabot, G. (1990), "Random particle model for fracture of aggregate or fiber composites", *J. Eng. Mech. - ASCE*, **116**(8), 1686-1705.
- Brekelmans, W.A.M. and Ayyapureddi, S. (1995), "Reduction of mesh sensitivity in continuum damage mechanics", *Acta Mech.*, **110**, 49-56.
- Bui, D.D., Hu, J. and Stroeven, P. (2005), "Particle size effect on the strength of rice husk ash blended gap-graded Portland cement concrete", *Cement Concrete Compos.*, **27**(3), 357-366.
- Carpinteri, A., Cornetti, P. and Puzzi, S. (2004), "A stereological analysis of aggregate grading and size effect on concrete tensile strength", *Int. J. Fract.*, **128**(1), 233-242.
- Chen, B. and Liu, J. (2004), "Effect of aggregate on the fracture behavior of high strength concrete", *Constr. Build. Mater.*, **18**(8), 585-590.
- Du, C.B. and Sun, L.G. (2007), "Numerical simulation of aggregate shapes of two-dimensional concrete and its application", *J. Aero. Eng.*, **20**(3), 172-178.
- Ferrara, L. and Di Prisco, M. (2001), "Mode I fracture behavior in concrete: nonlocal damage modelling", *J. Eng. Mech. - ASCE*, **127**(7), 678-692.
- Freudenthal, A.M. (1950), *The inelastic behaviour of engineering materials and structures*, Wiley, New York, USA.
- Goldman, A. and Bentur, A. (1993), "The influence of microfillers on enhancement of concrete strength", *Cement Concrete Res.*, **23**(4), 962-972.
- He, H. (2010), "Computational modelling of particle packing in concrete", PhD Thesis, Delft University of Technology, Delft.
- He, H., Guo, Z., Stroeven, P., Stroeven, M. and Sluys, L.J. (2009), "Influence of particle packing on elastic properties of concrete", *Computational Technologies in Concrete Structures* (Choi, C.K., Meyer, C. and Bicanic, N. (eds)), Techno-Press, Daejeon, 1177-1198.
- Herrmann, H.J., Hansen, A. and Roux, S. (1989), "Fracture of disordered, elastic lattices in two dimensions", *Phys. Rev. B*, **39**(1), 637-648.
- Hu, J. and Stroeven, P. (2004), "Properties of interfacial transition zone in model concrete", *Interface. Sci.*, **12**, 389-397.
- Jirásek, M. and Patzák, B. (2002), "Consistent tangent stiffness for nonlocal damage models", *Comput. Struct.*, **80**(14-15), 1279-1293.
- Jirásek, M. and Marfia, S. (2005), "Non-local damage model based on displacement averaging", *Int. J. Numer. Meth. Eng.*, **63**(1), 77-102.

- Kwan, A.K.H., Wang, Z.M. and Chan, H.C. (1999), "Mesoscopic study of concrete II: nonlinear finite element analysis", *Comput. Struct.*, **70**, 545-556.
- Leite, J.P.B., Slowik, V. and Mihashi, H. (2004), "Computer simulation of fracture processes of concrete using mesolevel models of lattice structures", *Cement Concrete Res.*, **34**(6), 1025-1033.
- Li, C.Q., Zheng, J.J., Zhou, X.Z. and McCarthy, M.J. (2003), "A numerical method for the prediction of elastic modulus of concrete", *Mag. Concrete Res.*, **55**(6), 497-505.
- Lilliu, G. (2007), "3D analysis of fracture processes in concrete", PhD Thesis, Delft University of Technology, Delft.
- Peerling, R.H.J. (1999), "Enhanced damage modeling for fracture and fatigue", PhD Thesis, Eindhoven University of Technology, Eindhoven.
- Radtke, F.K.F., Simone, A., Stroeven, M. and Sluys, L.J. (2008), "Multiscale framework to model fibre reinforced cementitious composite and study its microstructure", *Proceedings of International RILEM Symposium on Concrete Modelling - ConMod '08* (Schlangen E. and de Schutter G. (eds)), RILEM, Bagneux, 551-558.
- Rocco, C.G. and Elices, M. (2008), "Effect of aggregate size on the fracture and mechanical properties of a simple concrete", *Eng. Fract. Mech.*, **75**(13), 3839-3851.
- Rocco, C.G. and Elices, M. (2009), "Effect of aggregate shape on the mechanical properties of a simple concrete", *Eng. Fract. Mech.*, **76**(2), 286-298.
- Schlangen, E. and Garboczi, E.J. (1997), "Fracture simulations of concrete using lattice models: computational aspects", *Eng. Fract. Mech.*, **57**(2-3), 319-332.
- Scrivener, K.L. and Nemati, K.M. (1996), "The percolation of pore space in the cement paste/aggregate interfacial zone of concrete", *Cement Concrete Res.*, **26**(1), 35-40.
- Stock, A.F., Hannant, D.J. and Williams, R.I.T. (1979), "The effect of aggregate concentration upon the strength and modulus of elasticity of concrete", *Mag. Concrete Res.*, **31**, 225-234.
- Stroeven, P. (1973), "Some aspects of the micromechanics of concrete", PhD Thesis, Delft University of Technology, Delft.
- Stroeven, P., Hu, J. and Stroeven, M. (2009), "On the usefulness of discrete element computer modeling of particle packing for material characterization in concrete technology", *Comput. Concrete*, **6**(2), 133-153.
- Tabsh, S.W. and Abdelfatah, A.S. (2009), "Influence of recycled concrete aggregates on strength properties of concrete", *Constr. Build. Mater.*, **23**(2), 1163-1167.
- Tasdemir, M.A. and Karihaloo, B.L. (2001), "Effect of aggregate volume fraction on the fracture parameters of concrete: a meso-mechanical approach", *Mag. Concrete Res.*, **53**(6), 405-415.
- Tschegg, E.K., Elser, M. and Kreuzer, H. (1995), "Mode I fracture behaviour of concrete under biaxial loading", *J. Mater. Sci.*, **30**(1), 235-242.
- van Vliet, M.R.A. and van Mier, J.G.M. (1999), "Effect of strain gradients on the size effect of concrete in uniaxial tension", *Int. J. Fract.*, **95**(1-4), 195-219.
- Vonk, R.A. (1992), "Softening of concrete loaded in compression", PhD Thesis, Delft University of Technology, Delft.
- Wells, G.N. and Sluys, L.J. (2001), "A new method for modelling cohesive cracks using finite elements", *Int. J. Numer. Meth. Eng.*, **50**(12), 2667-2682.
- Yan, D. and Lin, G. (2006), "Dynamic properties of concrete in direct tension", *Cement Concrete Res.*, **36**(7), 1371-1378.
- Yaşar, E., Erdoğan, Y. and Kılıç, A. (2004), "Effect of limestone aggregate type and water-cement ratio on concrete strength", *Mater. Lett.*, **58**, 772-777.
- Zheng, J. (2000), "Mesostructure of concrete", PhD Thesis, Delft University Press, Delft.
- Zhou, X.Q. and Hao, H. (2008), "Mesoscale modelling of concrete tensile failure mechanism at high strain rates", *Comput. Struct.*, **86**(21-22), 2013-2026.

**Notations**

- $E$  and  $\mu$  : Young's modulus and Poisson's ratio, respectively  
 $\sigma_t$  : Tensile strength  
 $\sigma$  and  $\varepsilon$  : Stress and strain, respectively  
 $\mathbf{D}$  and  $\omega$  : Stiffness matrix of undamaged material and damage scalar, respectively  
 $\varepsilon_0$  and  $\varepsilon_f$  : Strain at peak stress and parameter specifying slope of softening branch  
 $k$  : Parameter related to history of damage evolution  
 $Y$  and  $\tilde{\varepsilon}$  : Damage energy release rate and equivalent strain, respectively  
 $\lambda$  and  $h$  : Width of damage zone and parameter related to element size, respectively